Lipid Abundance in Zebrafish Embryos Is Regulated by Complementary Actions of the Endocannabinoid System and Retinoic Acid Pathway

Daniel Fraher, Megan K. Ellis, Shona Morrison, Sean L. McGee, Alister C. Ward, Ken Walder, and Yann Gibert

Metabolic Research Unit, Deakin University School of Medicine, Geelong 3217, Australia

The endocannabinoid system (ECS) and retinoic acid (RA) signaling have been associated with influencing lipid metabolism. We hypothesized that modulation of these pathways could modify lipid abundance in developing vertebrates and that these pathways could have a combinatorial effect on lipid levels. Zebrafish embryos were exposed to chemical treatments altering the activity of the ECS and RA pathway. Embryos were stained with the neutral lipid dye Oil-Red-O (ORO) and underwent whole-mount in situ hybridization (WISH). Mouse 3T3-L1 fibroblasts were differentiated under exposure to RA-modulating chemicals and subsequently stained with ORO and analyzed for gene expression by qRT-PCR. ECS activation and RA exposure increased lipid abundance and the expression of lipoprotein lipase. In addition, RA treatment increased expression of CCAAT/enhancer-binding protein alpha. Both ECS receptors and RA receptor subtypes were separately involved in modulating lipid abundance. Finally, increased ECS or RA activity ameliorated the reduced lipid abundance caused by peroxisome proliferator–activated receptor gamma (PPARγ) inhibition. Therefore, the ECS and RA pathway influence lipid abundance in zebrafish embryos and have an additive effect when treated simultaneously. Furthermore, we demonstrated that these pathways act downstream or independently of PPARγ to influence lipid levels. Our study shows for the first time that the RA and ECS pathways have additive function in lipid abundance during vertebrate development. **(*Endocrinology* 156: 3596–3609, 2015)**

Obesity has become a global epidemic as it is estimated that greater than 500 million people worldwide are characterized as obese (1). Obese subjects are at a higher risk of developing medical conditions such as type 2 diabetes, cardiovascular disease, fatty liver disease, gall stones, or even cancer (2–5). However, current treatments for obesity are often ineffective in preventing long-term weight gain (3, 6). Therefore, it is essential to find effective treatments for this condition.

Here, we have focused on two signaling pathways that are associated with lipid metabolism, the endocannabinoid system (ECS) and the retinoic acid (RA) pathway. The ECS consists of two primary ligands, N-arachidonoylethanolamine (anandamide) and 2-arachinodonylglycerol (2-AG); and two definitive receptors, cannabinoid receptor type-1 (CB1) and cannabinoid receptor type-2 (CB2) (7–10). The presence of a putative third receptor remains controversial (11, 12). The ECS has previously been shown to be involved in lipid metabolism and adiposity independent of its well-known role in appetite regulation. For example, the adipose tissue of obese rats had increased CB1 expression (13). In addition, in vitro studies have shown that ECS activation increased lipid accumulation by increasing lipoprotein lipase activity (14), increasing peroxisome proliferator–activated receptor gamma (PPARγ) levels (15), and by decreasing the

ISSN Print 0013-7227 ISSN Online 1945-7170
Printed in USA
Copyright © 2015 by the Endocrine Society
Received April 8, 2015. Accepted July 9, 2015.
First Published Online July 16, 2015

Abbreviations: 2-AG, 2-arachinodonylglycerol; AM 630, selective CB2 inverse agonist; BADGE, bisphenol A diglycidyl ether; BMS 614, selective RARα antagonist; BMS 753, selective RARα agonist; BMS 961, selective RARγ agonist; C/ebpα, CCAAT/enhancer-binding protein alpha; CB1, cannabinoid receptor 1; CB2, cannabinoid receptor 2; CD 2665, Selective RARγ antagonist; DEAB, 4-diethylaminobenzaldehyde; dpf, days postfertilization; ECS, endocannabinoid system; Fabp11a, fatty acid binding protein 11a; hpf, hours post-fertilization; HU 308, selective CB2 agonist; Oleamide, selective CB1 agonist; ORO, Oil-Red-O; PPARγ, peroxisome proliferator–activated receptor gamma; Proxl, prospero-related homeobox I; RA, retinoic acid; RAR, retinoic acid receptor; Rimo, rimonabant (Selective CB1 inverse-agonist); Rosi, rosiglitazone; Win, (+)-WIN 55,212-2 mesylate; WISH, whole-mount in situ hybridization.

RIGHTSLINK
The Endocrine Society. Downloaded from press.endocrine.org by [${individualUser.displayName}] on 19 May 2016. at 16:09 For personal use only. No other uses without permission. . All rights reserved.

expression of adiponectin (16), an adipokine associated with reducing lipid accumulation. Furthermore, circulating 2-AG levels were higher in human obese subjects than in lean subjects (17).

RA is the major active derivative of vitamin A (retinol) (18). Retinol is converted into retinaldehyde by the actions of alcohol dehydrogenases or retinol dehydrogenases. Retinaldehyde is in turn converted to RA by retinaldehyde dehydrogenase. RA is a small molecule that can easily pass through the cell membrane, being subsequently transported to the nucleus by cellular RA-binding proteins where it binds the nuclear receptors, retinoic acid receptors (RARs) (19, 20). These activated RARs influence transcription by binding directly to DNA. Levels of RA are regulated by its production via this process or degradation by CYP26 enzymes (21). The exact role of RA signaling in adiposity remains unclear. Several studies have reported that RA decreased lipid abundances in both mice (22–24) in cell lines (25, 26). However, complicating the effects of RA on lipid metabolism, a study reported that RA increased adiposity in rats (27) and other cell line studies have shown that RA increased the differentiation of adipocytes (28, 29). The increase of adiposity caused by RA more closely resembles the outcome observed in humans, in which treatment has been shown to increase body weight, a common adverse effect associated with RA syndrome (30).

Zebrafish (*Danio rerio*) have become a common and relevant model for the study of lipid biology (31–33). Importantly, many aspects of lipid metabolism and associated genes are conserved between zebrafish and humans (34). Zebrafish also have very low-density lipoproteins, low-density lipoproteins, high-density lipoproteins and the major classes of apolipoproteins (reviewed by Schlegel and Gut) (35). A key advantage of studying zebrafish embryos is that during development, the embryos rely on a yolk for nutrition, eliminating any potential dietary variables. These attributes make the zebrafish an ideal model for studying lipid biology and for identifying potential therapeutic targets.

Here, we aim to determine how modulations of the ECS or RA pathways affect lipid deposition and the expression of lipid-associated genes during zebrafish embryogenesis. We demonstrate that both pathways can reduce lipid levels and identify for the first time an additive effect of the ECS and RA pathway on lipid abundance. In addition, we establish the specific receptors for each pathway are involved in influencing lipid deposition during embryogenesis, notably identifying a role for CB2 activity, which has not previously been directly associated with regulating lipid accumulation in vivo. Therefore, we propose that the abilities of these pathways to influence lipid abundance at the receptor level provide ideal targets for obesity therapeutics. To further understand the position of the ECS and RA pathway within the signaling cascades controlling lipid levels, we blocked the activity of PPARγ, a critical gene involved in multiple aspects of lipid metabolism, including stimulating fatty acid transport and lipoprotein lipase (*Lpl*) expression (36, 37). Cotreatment with either an ECS activator or exogenous RA was sufficient to restore the decreased lipid abundance caused by PPARγ inhibition, indicating that these pathways act either downstream or independently of PPARγ signaling. This work points to potential therapeutic targets for the treatment of obesity. Importantly, the additive effects suggest that combinational approaches might alleviate possible harmful off-target effects caused by treatments that alter the pathways.

Materials and Methods

Experimental animals

Zebrafish were reared and staged at 28.5°C in E3 embryo media according to Kimmel et al (38). All zebrafish studies were approved by the Deakin University Animal Welfare Committee (AWC 81–2011).

Oil-Red-O staining

Embryos were stained with Oil-Red-O (ORO) according to a protocol adapted from Schlegel et al (33). Staining occurred for 75 minutes followed by two 10-minute rinses in 60% 2-propanol. Representative embryos were used for photography, $n > 25$, replicated at least twice. Widths of ORO bands were measured using Cell Sens Dimension (Olympus). Statistical analysis was performed using IBM SPSS Statistics version 21. Comparisons were made with an Independent Samples *t* test, significance was applied when $P < .05$; $n = 7$. Due to low sample sizes in some instances, nonparametric statistical analysis was performed for this experiment and subsequent experimental analyses. A Kruskal-Wallis test was performed to assess differences in groups ($P < .001$). Cases were selected and were run through a Mann-Whitney *U* Test and significance was assessed at $P < .05$. Nonparametric statistical analysis closely reflected the results obtained using Independent Samples *t* tests; therefore, significance was determined according to Independent Samples *t* tests.

Whole-mount in situ hybridization

Embryos were fixed in 4% PFA-PBS overnight at 4°C and then transferred to and stored in 100% methanol at −20°C. Whole-mount in situ hybridization using digoxigenin-labeled riboprobes was performed as described (39). The following probes were used: CCAAT/enhancer-binding protein alpha (40), fatty acid–binding protein 11a (41), lipoprotein lipase (41), peroxisome proliferator–activated receptor gamma (42), prosper homeobox 1 (43), retinaldehyde dehydrogenase 2 (44), cannabinoid receptor 1 (45), and cytochrome P450 26a1 (46). Area of expression was measured using Cell Sens Dimension (Olympus). Statistical analysis was performed using IBM SPSS Statistics ver-

RIGHTSLINK
The Endocrine Society. Downloaded from press.endocrine.org by [${individualUser.displayName}] on 19 May 2016. at 16:09 For personal use only. No other uses without permission. . All rights reserved.

sion 21. Comparisons were made with an Independent Samples *t* test, significance was applied when $P < .05$; $n > 5$; replicated at least twice.

Quantitative real-time PCR analysis

Total RNA was extracted from cells using RNeasy columns (QIAGEN). cDNA was generated from total RNA using Superscript First-Strand Synthesis System for RT-PCR (Invitrogen Life Technologies). Gene expression levels were measured using FastStart Universal SYBR Green Master (Roche Australia) on an Mx3005P cycler (Stratagene), and cDNA concentration was normalized to OliGreen using a Quant-iT OliGreen ssDNA Assay Kit (Invitrogen).

Chemical treatments

(+)-WIN 55,212-2 mesylate (Win), Rimonabant (Rimo), 4-diethylaminobenzaldehyde (DEAB), BMS 753, BMS 614, BMS 961, CD 2665, oleamide, AM 630, bisphenol A diglycidyl ether (BADGE), and Rosiglitazone (Rosi) were dissolved into dimethyl sulfoxide in a stock solution of 10mM. RA and HU 308 were dissolved into ethanol in a stock solution of 100mM and 10mM, respectively. Solutions were stored at −20°C. Embryos were placed into 25 mL of E3 medium in 50-mL tubes. Appropriate volumes of chemicals were added directly to the medium and tubes were placed horizontally in an incubator at 28.5°C. BMS 753, BMS 614, BMS 961, CD 2665, oleamide and AM 630 were purchased from Tocris Bioscience (Bristol). Rimo was purchased from Cayman Chemical; DEAB, BADGE, and RA were purchased from Sigma-Aldrich. Rosi was purchased from Molekula Limited. A dose response was performed for each chemical to assess the appropriate concentration so that there were no toxic effects on the embryos.

Cell Culture

Mouse 3T3-L1 fibroblasts were cultured in 10% CO_2 at 37°C in growth media consisting of DMEM (4.5 g/L glucose; Invitrogen), 10% (v/v) heat-inactivated fetal bovine serum (Thermo Scientific), and antibiotics (100 U/mL penicillin and 100 mg/mL streptomycin; Life Technologies). Cells were induced to differentiate 3 days after reaching confluence (day 0), by supplementing growth media with 4nM insulin (Humulin; Eli Lilly), 0.25mM dexamethasone (Sigma-Aldrich) and 0.5mM 1-methyl-3-isobutyl-xanthine (Sigma-Aldrich). Differentiation media was refreshed every 2 days during differentiation. At 4 and 7 days post differentiation, cells were treated with growth media plus insulin only. At 9 days post differentiation, cells were treated with only growth media. Cell treatments began 3 days prior to differentiation and continued through to 10 days post differentiation. Treatments were refreshed when growth media was changed. Rosi and berberine were used at 10μM and 3μM, respectively. The 3T3-L1 cell line was authenticated by phenotypic and genotypic analysis and the ability to differentiate into adipocytes (performed February 2015). We extracted the ORO by incubating cells in 100% isopropanol for 15 minutes. We then removed the supernatant and placed it into a 96-well plate and read absorbance at 492nM using a Bio-Rad xMark Microplate Spectrophotometer.

Mitochondria staining

Mitotracker Deep Red FM (Invitrogen) stock solution was prepared by dissolving 50 μg into 94 μL of dimethyl sulfoxide. Stock solution was stored in the dark at −20°C. Embryos were treated with a working solution of 4 μL stock solution dissolved into 10 mL of embryo media in the dark for 2 hours at 28.5°C. Embryos were assessed for fluorescent puncta, labeling mitochondria, using a UV source with an red fluorescent protein filter.

Oxygen consumption assay

Oxygen consumption rate was assessed using the Seahorse XF24 Flux Analyzer (Seahorse Bioscience). Embryos were placed into a 24-well XF24 islet capture microplate and analyzed at 28.5°C. Basal rate measurements were performed in triplicate (at 5-min intervals) and three maximal rates were measured following exposure to 1μM carbonyl cyanide-4-(trifluoromethoxy)phenylhydrazone (Sigma-Aldrich).

Results

ECS and RA pathway influence lipid abundance in developing zebrafish embryos

Treatment with the CB1 and CB2 agonist (+)-WIN 55,212-2 mesylate (Win), the CB1 inverse agonist Rimo, exogenous RA, and the RA synthesis inhibitor DEAB from 26 hours post fertilization (hpf) until 55 hpf were used to modify the activity of the ECS and RA pathway in zebrafish embryos. This timing of treatment was chosen because it coincides with the initial detection of neutral lipids in the developing embryo, but is late enough in embryogenesis to avoid potential developmental effects; doses were determined by performing a dose response (Supplemental Table 1). To determine the amount of lipid present in developing zebrafish embryos, fish were stained with Oil-Red-O (ORO), a stain of neutral lipids. In control embryos, the stain was located in the forebrain, around the eye, underneath the otic vesicle, and in the developing vasculature (Figure 1A–C; blue and black brackets, arrowhead, arrow). Exposure to 6nM RA expanded the localization and produced a more dense ORO stain in these areas (Figure 1, D–F; blue and black brackets, arrowhead, arrow), whereas blocking the production of RA with 10μM DEAB reduced lipid amounts to diffuse spots above the eye and completely absent posterior to the eye (Figure 1, G–I, pound sign, arrowhead, arrow). Similarly, increasing ECS activity with treatment with 0.3μM Win caused an expansion of the stained area and a more intense ORO staining (Figure 1, J–L; blue and black brackets, arrowhead, arrow) and decreasing ECS activity with 3μM Rimo decreased the area and intensity of ORO staining in the embryos (Figure 1, M–O; blue and black bracket, arrowhead, arrow). To further assess the expansion or decrease

RIGHTSLINK
The Endocrine Society. Downloaded from press.endocrine.org by [${individualUser.displayName}] on 19 May 2016. at 16:09 For personal use only. No other uses without permission. . All rights reserved.

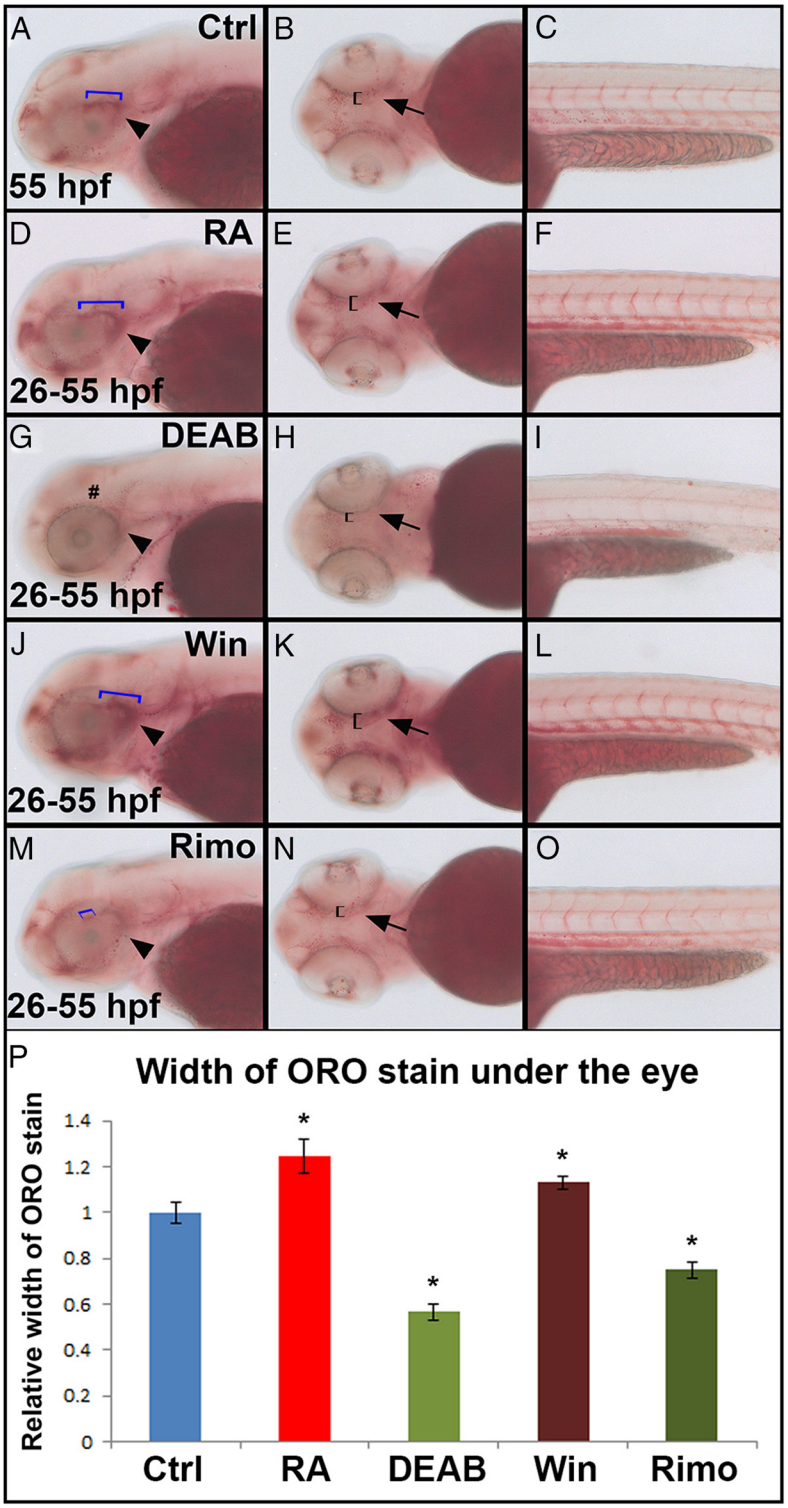

Figure 1. The effects of modulating RA signaling and the ECS on lipid abundance. Embryos treated from 26–55 hpf with 6nM RA (D–F) showed expanded and denser ORO stain around the eye (blue and black brackets, arrow, arrowhead) and in the vasculature (F) whereas embryos treated with 10μM DEAB (G–I) showed decreased ORO (black brackets, arrow, arrowhead) and an absent domain of ORO stain (pound sign) compared with control embryos (A–C). Embryos treated with 0.3μM Win (J–L) showed increased ORO stain (blue and black brackets, arrow, arrowhead) and embryos treated with 3μM Rimo (M–O) showed decreased ORO stain (blue and black brackets, arrow, arrowhead). The width of the bands of ORO stain under the eye was measured (P, black brackets). RA- and Win-treated embryos had significantly higher widths of bands, whereas DEAB- and Rimo-treated embryos had significantly lower band widths. *, $P < .05$.

of the area of ORO staining, the width of the ORO-stained bands located below the eye were measured (Figure 1P). Fitting with the observed changes of overall ORO stain previously described, RA- and Win-treated embryos showed a larger width of the ORO band below the eye, whereas DEAB- and Rimo-treated embryos had bands that were decreased in size (Figure 1P). To confirm that the decreases in ORO stain caused by DEAB and Rimo treatment were not due to toxic effects, we modulated the pathways with both the activators and the inhibitors (ie, an RA + DEAB or Win + Rimo treatment). Because two full treatments of the pathways would cause toxic effects, we performed combined doses at concentrations below the full treatments. A combined 50% dose of RA and DEAB or combined 60% dose of Win and Rimo did not affect lipid deposition in the treated embryos (Supplemental Figure 1, A–F). Therefore, we conclude that the ECS and RA pathway have roles in modulating lipid abundance during embryogenesis.

Expression of genes associated with lipid metabolism are altered by ECS- and RA-signaling modulation

To further examine the effects that the ECS and the RA pathway have on lipid metabolism in the developing embryo, we analyzed the expression of metabolic- and lipid-associated genes using WISH. A later window of treatment, from 50 to 72 hpf, was chosen because the relevant genes are more highly and broadly expressed during this period. Given that a later timing of treatment was selected, the dosage of treatments needed to be increased to maintain effectiveness in the older embryos. We observed that the expression of *lpl*, a gene involved in processing lipids contained within lipoproteins,

RIGHTSLINK
The Endocrine Society. Downloaded from press.endocrine.org by [${individualUser.displayName}] on 19 May 2016. at 16:09 For personal use only. No other uses without permission. . All rights reserved.

was altered by the modulation of the pathways. In embryos treated with 10nM RA from 50 to 72 hpf, *lpl* expression was increased (Figure 2B), whereas 15μM DEAB treatment decreased *lpl* expression (Figure 2D). In addition, embryos exposed to 0.4μM Win showed an increase in *lpl* expression (Figure 2J) whereas those exposed to 4μM Rimo showed a decrease (Figure 2L). Given that *lpl* was expressed primarily in liver, we wanted to account for potential effects on liver size from our chemical treatments. Therefore, we analyzed the expression of *proxI*, a transcription factor expressed in developing hepatocytes of zebrafish (47, 48). The expression of *proxI* was not altered by any of the treatments (Figure 2, F, H, N, and P). Changes in *lpl* and *proxI* expression were quantified by measuring the area of staining from WISH. RA-treated embryos showed a trend of increase in *lpl* expression whereas DEAB-treated embryos showed a significant decrease (Figure 2Q). Embryos treated with Win showed a significant increase in *lpl* expression whereas embryos treated with Rimo showed a decrease (Figure 2S). The expression of *proxI* was not changed by any of the treatments (Figure 2, R and T). The expression of CCAAT/enhancer-binding protein alpha (*c/ebpα*), a transcription factor that regulates energy homeostasis and adipogenesis (49, 50), was increased in embryos treated with 10nM RA and decreased with 15μM DEAB treatment (Figure 2, V and X). Furthermore, fatty acid–binding protein 11a (*fabp11a*), a gene involved in lipid mobilization, was more highly expressed in embryos treated with 10nM RA and had lower expression in embryos treated with 15μM DEAB (Figure 2, D′ and F′). However, embryos treated with 0.4μM Win or 4μM Rimo did not exhibit a change of *c/ebpα* or *fabp11a* expression compared with controls (Figure 2, Y–B′, G′–J′).

Given that alteration of ECS and RA signaling resulted in modified lipid accumulation and gene expression, it was important to assess the metabolic activity of the embryos. Fluorescently staining the mitochondria of embryos revealed that the treatments did not change the number of mitochondria (Supplemental Figure 2, A–E). In addition, no effect on the oxygen consumption rate of embryos was

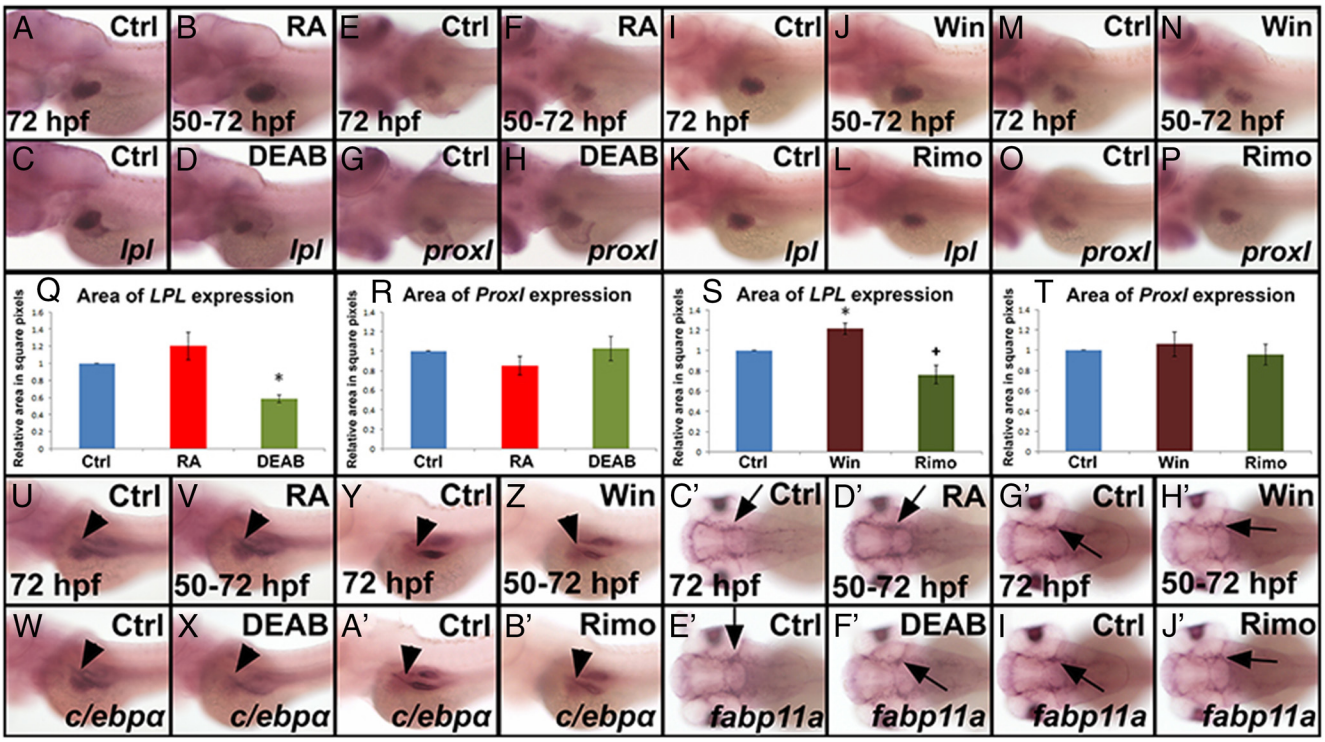

Figure 2. RA signaling and the ECS influence genes associated with lipid metabolism. Embryos treated from 50–72 hpf with 10nM RA (B) showed increased area of *lpl* expression, whereas embryos treated with 15μM DEAB (D) showed decreased expression compared with control embryos (A and C). E–H, These treatments did not alter the expression of *proxI*. Embryos treated with 0.4μM Win (J) showed increased area of *lpl* expression whereas embryos treated with 4μM Rimo (L) showed decreased expression compared with control embryos (I and K). M–P, These treatments did not modify *proxI* expression. Q–T, Measuring the relative area of expression in square pixels supported altered expression trends that were observed. Embryos treated from 50–72 hpf with 10nM RA showed increased area of *c/ebpα* expression (V, arrowhead), whereas embryos treated with 15μM DEAB showed decreased expression (X compared with U and W) control embryos. Embryos treated with 0.4μM Win or 4 μM Rimo did not show changed *c/ebpα* expression compared with controls (Y–B′). Embryos treated from 50–72 hpf with 10nM RA showed increased area of *fabp11a* expression (Z, arrow), whereas embryos treated with 15μM DEAB showed decreased expression (B′ arrow) compared with (Y and A′, arrow) control embryos. Win- or Rimo-treated embryos did not show a change in *fabp11a* expression (G′–J′).

RIGHTSLINK
The Endocrine Society. Downloaded from press.endocrine.org by [${individualUser.displayName}] on 19 May 2016. at 16:09 For personal use only. No other uses without permission. . All rights reserved.

observed at either basal or maximal respiratory capacities following treatment (Supplemental Figure 2, F and G).

CB1, CB2, RARα, and RARγ receptors influence lipid deposition

Zebrafish possess two RAR subtypes, RARα and RARγ, but there is no RARβ in the zebrafish genome. To determine the relative influence of each subtype on lipid deposition, embryos were treated with 0.03μM BMS 753 (selective RARα agonist), 0.4μM BMS 614 (selective RARα antagonist), 0.25μM BMS 961 (selective RARγ agonist), or 8μM CD 2665 (selective RARγ antagonist) from 26 to 55 hpf and stained with ORO. Treatment with the RARα agonist increased the area of ORO staining (Figure 3, E and F; arrowhead, bracket, arrow), whereas treatment with the RARα antagonist decreased the density and area of ORO staining (Figure 3, I and J; arrowhead, bracket, arrow). Treatment with the RARγ agonist or antagonist showed similar effects on lipid deposition as the RARα-specific modulators, but these effects were not as strong as in the embryos exposed to RARα (Figure 3, M, N, Q, and R; arrowhead, bracket, arrow). To identify the influence of each of the ECS receptors on lipid abundance, we treated embryos from 26 to 55 hpf with 3.5μM oleamide (selective CB1 agonist), 3μM Rimo (a selective CB1 inverse agonist), 3.5μM HU 308 (a selective CB2 agonist),

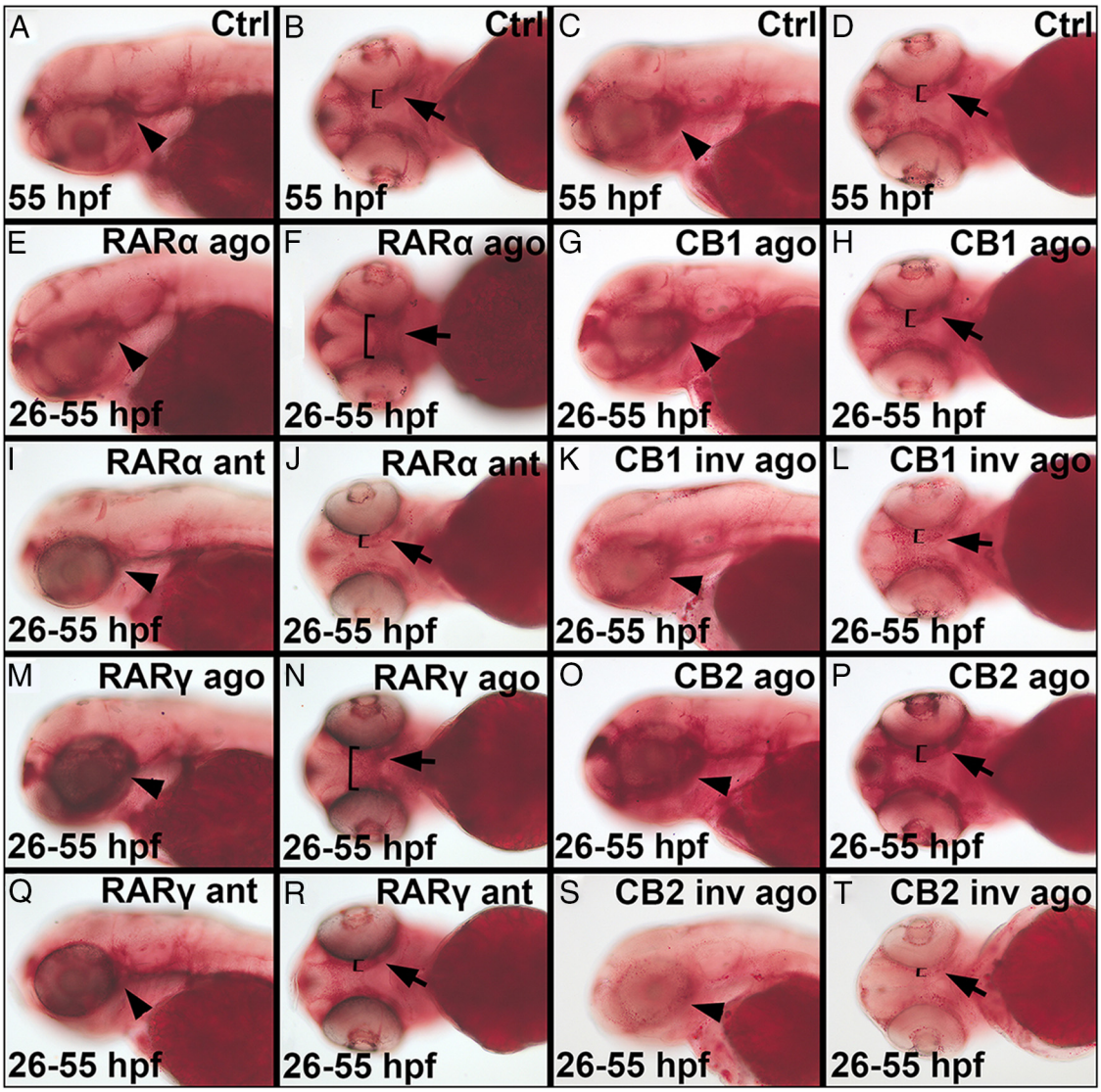

Figure 3. Modulation of RARs and cannabinoid receptors alter lipid levels in zebrafish embryos. (E, arrowhead; F, arrow, bracket) Treatment with the RARα agonist (0.03μM BMS 753) from 26–55 hpf increased ORO stain, whereas treatment with the RARα antagonist (0.4 μM BMS 614) (I and J) decreased ORO stain compared with control embryos (A and B). M and N, Treatment with the RARγ agonist (0.25μM BMS 961) from 26–55 hpf increased ORO stain, whereas treatment with the RARγ antagonist (8 μM CD 2665) (Q and R) decreased ORO stain. Treatment with the CB1 agonist (3.5μM oleamide) (G and H) from 26–55 hpf increased ORO stain, whereas treatment with the CB1 inverse agonist (3μM Rimo) (K and L) decreased ORO stain compared with control embryos (C and D). Treatment with the CB2 agonist (3.5 μM HU 308) (O and P) from 26–55 hpf increased ORO stain, whereas treatment with the CB2 inverse agonist (3.5μM AM 630) (S and T) decreased ORO stain.

RIGHTSLINK
The Endocrine Society. Downloaded from press.endocrine.org by [${individualUser.displayName}] on 19 May 2016. at 16:09 For personal use only. No other uses without permission. . All rights reserved.

or 3.5μM AM 630 (a selective CB2 inverse agonist) and stained with ORO. Both of the CB1 and CB2 agonists showed a moderate expansion of the lipid deposition, whereas they both increased the intensity of ORO stain, with the CB2 agonist–treated embryos having a strong increase (Figure 3, G, H, K, L, O, P, S, and T; arrowhead, bracket, arrow). This suggests that both CB and RA receptors influence lipid abundance during embryogenesis.

Increased ECS or RA signaling reversed the effects of modulating PPARγ signaling

PPARγ is an essential component of adipose development (36), so we sought to determine potential interactions between the ECS and/or RA pathways and *pparγ*. Modulation of the ECS and RA pathway did not affect the expression of *pparγ* during embryonic development (Supplemental Figure 3). When embryos were treated with 4μM bisphenol A diglycidyl ether (BADGE), a PPARγ antagonist (51) from 26 to 55 hpf, a decrease in ORO staining was detected (Figure 4, C and D). Embryos that were treated with both 4μM BADGE and 5nM RA or 0.3μM Win had higher ORO staining compared with BADGE-alone-treated embryos, a level of staining comparable to control embryos (Figure 4, E–H). Furthermore, under the same conditions, *lpl* expression was reduced in BADGE-treated embryos and this effect was ameliorated by concurrent treatment with RA or Win (Figure 4, K–L and Q). Furthermore, we increased PPARγ activity with the agonist Rosi. We performed a dose response and determined that 10μM Rosi increased *lpl* expression in embryos treated from 26 to 55 hpf (Figure 4, N and M). When embryos were treated with both 10μM Rosi and 10μM DEAB or 3μM Rimo, the expression of *lpl* returned back to the level of control embryos (Figure 4, M–P and R). We also observed an increase in *c/ebpα* expression in embryos treated with Win or RA and BADGE compared with embryos treated only with BADGE (data not shown). These data suggest that the ECS and RA pathway can rescue a lack of a functional or decreased overactive PPARγ signaling and that they act either downstream or independently of PPARγ in controlling lipid abundance.

RA inhibits adipocyte differentiation in adult mammalian 3T3-L1 fibroblasts

Our embryological data clearly points to an effect from RA in increasing lipid abundance (Figures 1–4). Therefore, we decided to investigate the influence of RA on adipocyte differentiation. Several authors have published conflicting data regarding the role of RA in adult adipocyte differentiation (23, 25, 28, 29). Much of the confusion stems from varying effects caused by RA in different experimental designs, possibly due to temporal alterations in RA signaling to act as a pro- or antiadipogenic agent (28). To tackle these apparent opposing results, we explored the influence of RA signaling on adipocyte differentiation within the context of a mature cell model to compare with our embryonic zebrafish model.

Therefore, we differentiated mouse 3T3-L1 fibroblasts under RA and DEAB exposure. We chose a mammalian cell model to expand the relevance of the data and because mouse 3T3-L1 fibroblasts are an established cell line for adipocyte differentiation. Cells were continually treated from 3 days prior to differentiation to 10 days post differentiation, when they were stained with ORO (Figure 5A). Vehicle control cells showed spherical morphology and high ORO staining (Figure 5B). Cells treated with 10μM DEAB or the positive control, Rosi, both had high levels of ORO stain comparable with vehicle cells (Figure 5, C and E). Cells treated with 1μM RA or the negative control, berberine, showed reduced ORO staining (Figure 5, D and F). Quantification of ORO stains revealed that RA and berberine decreased ORO staining to approximately 25 and 26% of vehicle-treated cells, respectively (Figure 5G). Furthermore, RA decreased the expression of *Lpl*, *C/ebpα*, *C/ebpβ1*, and *Pparγ*, whereas DEAB increased the expression of these genes (Figure 5, H–K). These results suggest that RA signaling inhibits differentiation of adipocytes in mature cell types when treatment is prior to differentiation, contrary to the effects on lipid abundance observed during embryogenesis.

Combined suboptimal doses of ECS and RA modulators have additive effects on lipid abundance in developing zebrafish embryos

Given that modulation of both the ECS and RA signaling influenced lipid abundance in zebrafish embryos, we investigated the effects of combining treatments. To establish complimentary actions of the two pathways, embryos were treated at a 60% dosage of full treatments, which were the doses used in the previous ORO experiment from 26 to 55 hpf (RA, 6nM, Win, 0.3μM, and Rimo, 3μM), except for DEAB, which had to be reduced because the 60% dosage still decreased ORO stain, so a full dose of DEAB was 5μM. The 60% treatments were chosen because they were low enough that chemical exposure to an individual treatment did not influence lipid deposition on its own and combined doses did not cause developmental delays or have toxic effects on the embryos; these were considered suboptimal doses. Embryos treated with 60% doses of Win and RA (Figure 6, C and E) did not show a change in lipid deposition compared with control embryos (Figure 6A), whereas the full doses increased ORO staining as we previously observed (Figure 6, B and D). However, combined 60% doses of Win and RA in-

RIGHTSLINK
The Endocrine Society. Downloaded from press.endocrine.org by [${individualUser.displayName}] on 19 May 2016. at 16:09 For personal use only. No other uses without permission. . All rights reserved.

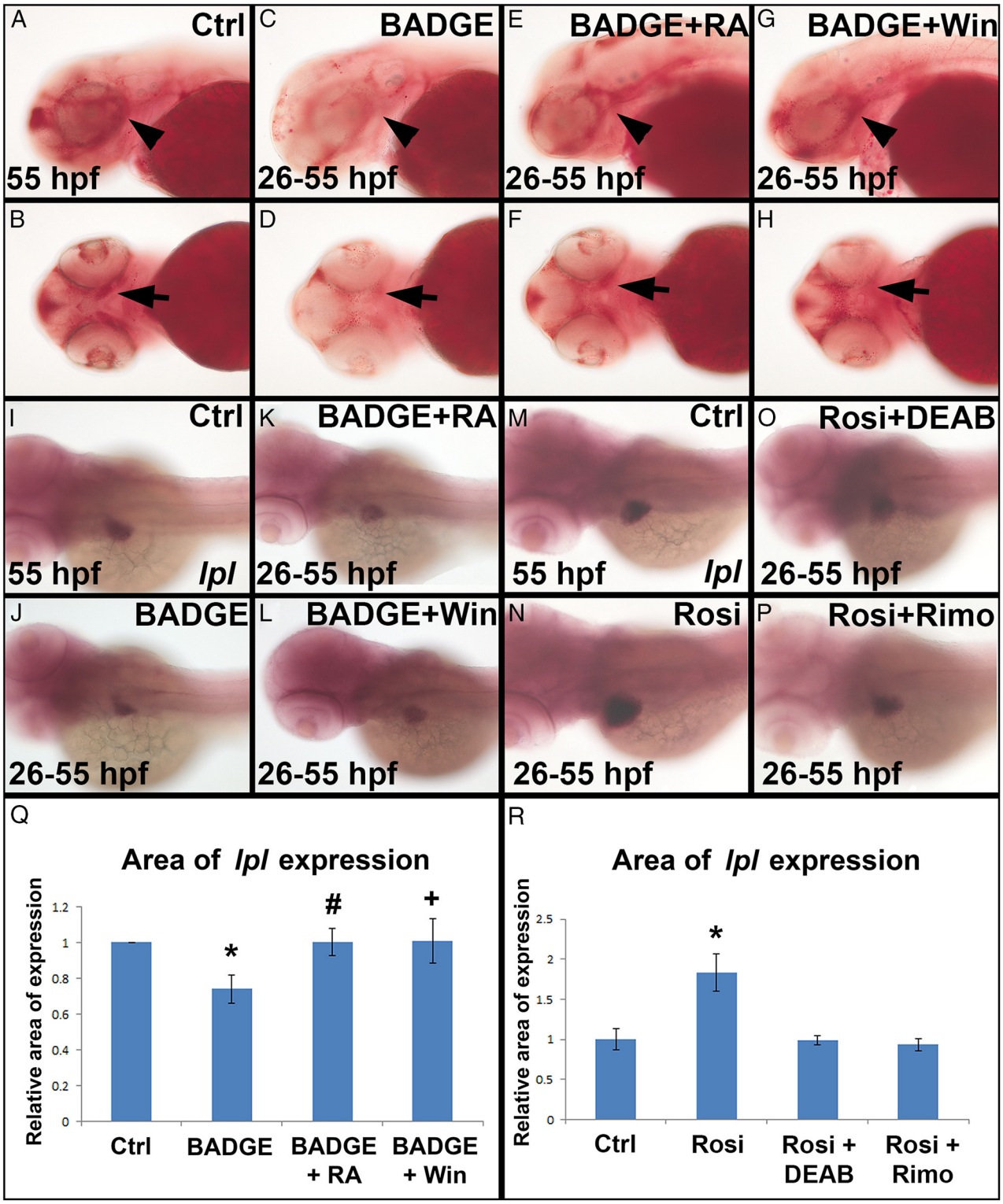

Figure 4. Exogenous RA and ECS activation ameliorates the effects from modulating PPARγ activity. C and D, Treatment with 4μM BADGE from 26–55 hpf reduced ORO stain compared with control embryos (A and B). Embryos treated with 4μM BADGE and 5nM RA (E and F) or 4μM BADGE and 0.3μM Win (G and H) showed a level of ORO stain higher than the BADGE-alone treated embryos, more comparable with control embryos. J, Embryos treated with 4μM BADGE had reduced *lpl* expression compared with control embryos (I). Embryos treated with 4μM BADGE and 5nM RA (K) or 4μM BADGE and 0.3μM Win (L) had a restored expression of *lpl*. Q, BADGE-treated embryos had a reduced area of *lpl* expression compared with control embryos, which was restored with treatment RA or Win. N, Embryos treated with 10μM Rosi had increased *lpl* expression compared with controls (M). O and P, Embryos treated with 10μM Rosi and 10μM DEAB or 3μM Rimo had *lpl* expression comparable to controls. R, Area of *lpl* expression was significantly increased in Rosi-treated embryos, whereas it was unchanged in Rosi-and–DEAB- or Rimo-treated embryos. *, $P < .05$ compared with control; #, $P < .05$ compared with BADGE treatment; +, $P = .074$ compared with BADGE treatment.

RIGHTSLINK
The Endocrine Society. Downloaded from press.endocrine.org by [${individualUser.displayName}] on 19 May 2016. at 16:09 For personal use only. No other uses without permission. . All rights reserved.

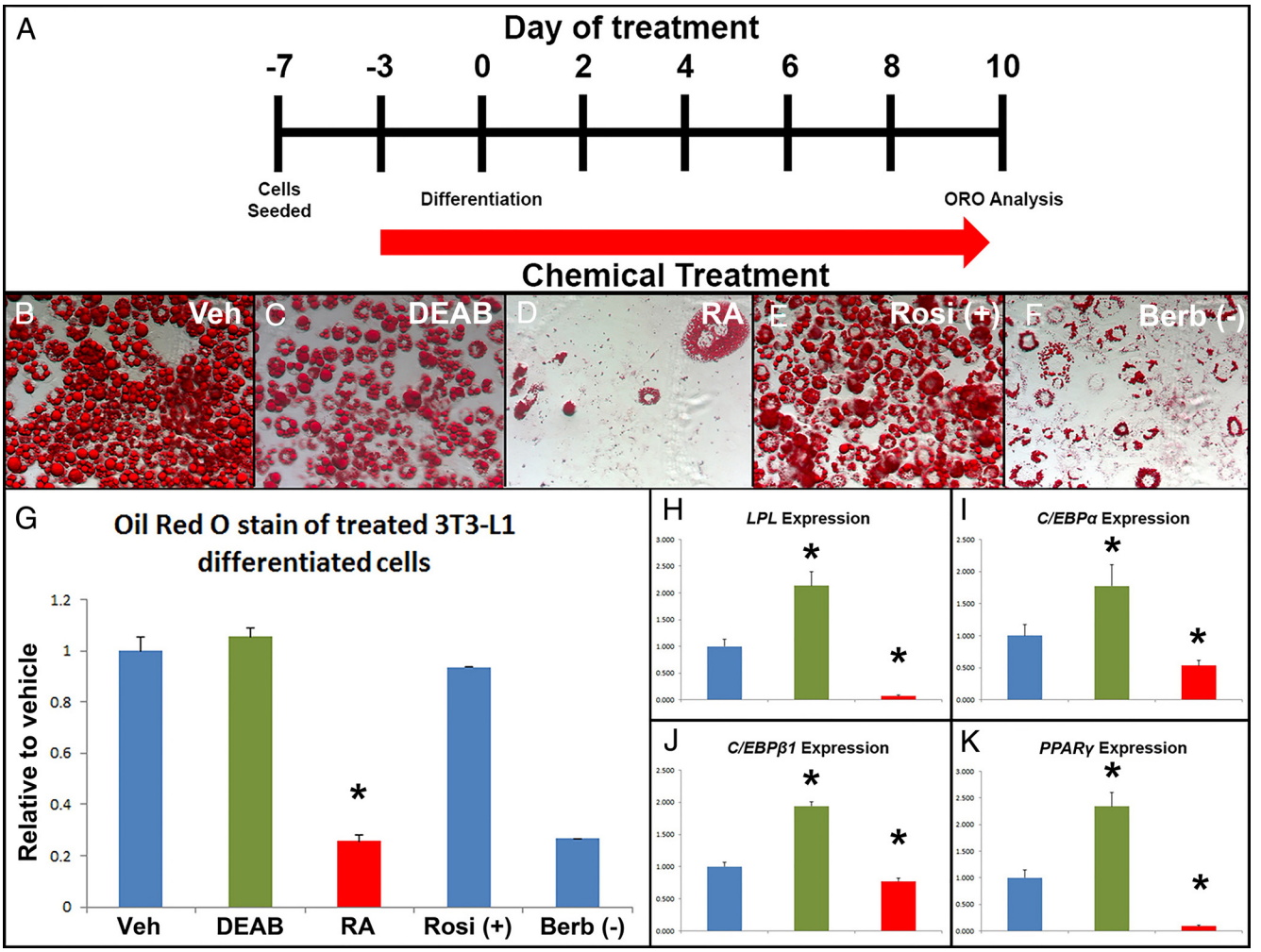

Figure 5. RA signaling influences adipocyte differentiation. (A) Timing of treatment: treatment of cells began 4 days after seeding and 3 days before differentiation was initiated. Treatment was given for 10 days. B–F, Mouse 3T3–L1 fibroblasts were stained with ORO after 10 days of differentiation treatment and 13 days of chemical treatment. C, Cells treated with 10μM DEAB had similar amounts of ORO to control cells (B) and 10μM Rosi-treated positive control cells (E). D, 1μM RA-treated cells had a much reduced ORO stain, which was similar to the 3μM berberine-treated negative control cells (F). G, Quantification of ORO shows a significantly decreased amount of lipid in RA and berberine-treated cells. Quantitative RT-PCR showed that DEAB increased the expression of *Lpl* (H), *C/ebpα* (I), *C/ebpβ1* (J), and *Pparγ* (K), whereas RA treatment decreased expression of the genes.

creased ORO staining in the embryos (Figure 6F). Similarly, the combined 60% Rimo and DEAB doses were sufficient to decrease lipid deposition compared with control embryos, similar to the full doses, that was not seen when embryos were treated with a 60% dose of only one of the chemicals (Figure 6, G–L). The area of expression of *lpl* was measured after treatment with the corresponding 60% doses of RA (full dose, 10nM), Win (full dose, 0.4μM) and Rimo (full dose, 4μM) from 50 to 72 hpf. A 50% dose of DEAB (full dose, 15μM) was used as a suboptimal treatment because a DEAB 60% dose was still sufficient to reduce *lpl* expression. These treatments revealed that the combined 60% treatment with Win and RA increased expression whereas the 60% doses alone did not (Figure 6M). The combined 60% dose of Rimo and 50% dose of DEAB was sufficient to decrease *lpl* expression in embryos but the individual treatment did not decrease expression (Figure 6N). To assess a synergistic effect, the area of *lpl* expression was measured in embryos that were treated with combined full doses (Figure 6, M and N). The full combination treatments were still significantly different from controls, but were not significantly different from the combination treatments. This reveals an additive effect, and not a synergistic effect, of the two pathways.

To determine whether there were interactions between the two pathways, we monitored the expression of genes in one pathway while modulating the other. RA activity can be indirectly observed by measuring the expression of *aldh1a2*, an enzyme involved in RA production, or

RIGHTSLINK
The Endocrine Society. Downloaded from press.endocrine.org by [${individualUser.displayName}] on 19 May 2016. at 16:09 For personal use only. No other uses without permission. . All rights reserved.

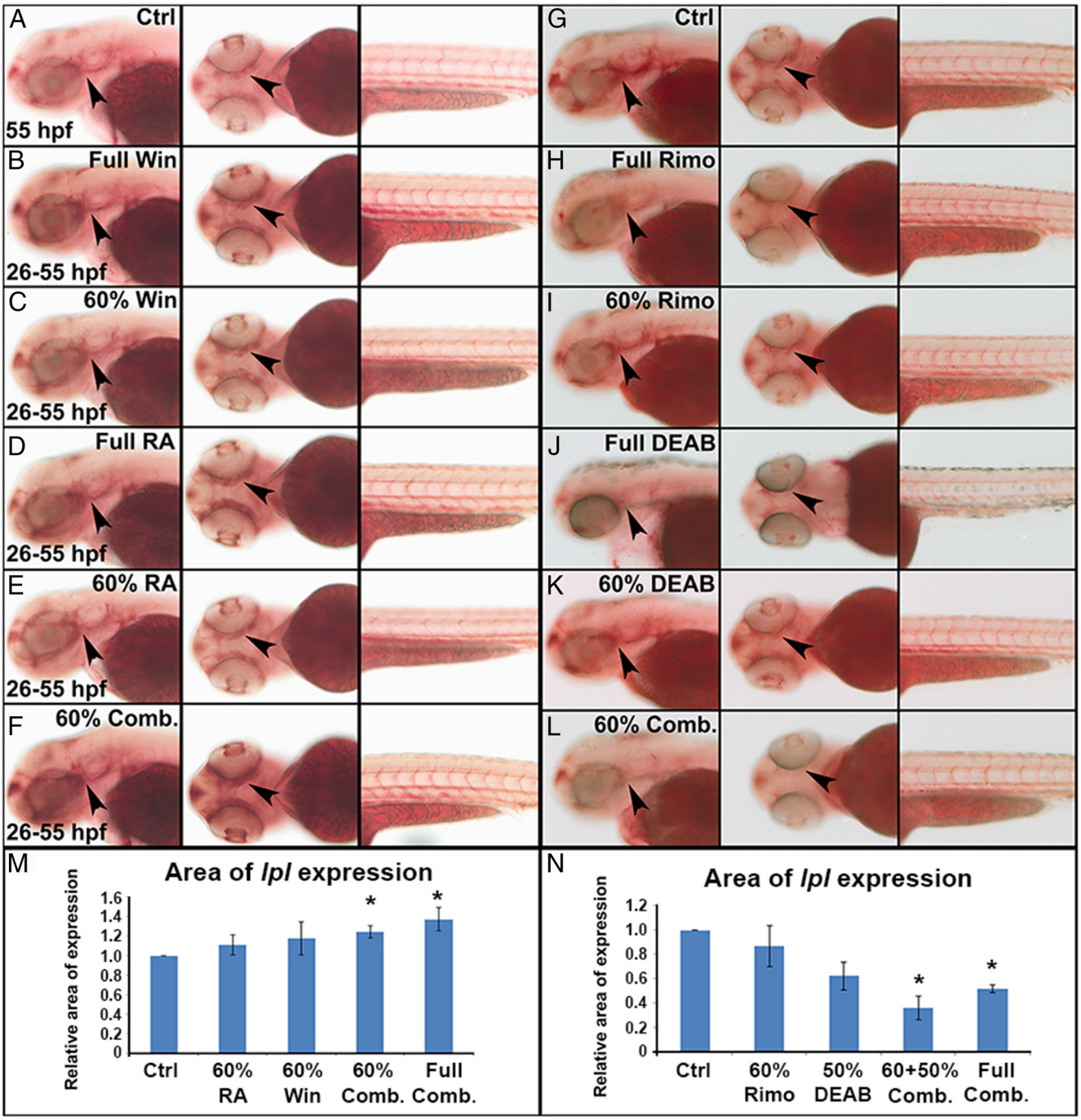

Figure 6. RA signaling and the ECS show combinatorial effects. (B) A full dose of Win from 26–55 hpf increased ORO stain, whereas a 60% dose (C) had no effect compared with control embryos (A). D, Full RA treatment increased ORO stain, whereas a 60% dose (E) had no effect. F, A combined 60% dose of the both Win and RA caused an increase in ORO stain. H, A full dose of Rimo decreased ORO stain, whereas a 60% dose (I) showed no effect compared with control embryos (G). J, A full dose of DEAB treatment decreased ORO stain, whereas a 60% dose (K) showed no effect on ORO stain. L, A combined 60% dose of Rimo and DEAB showed a decrease in ORO stain. M, Combined 60% doses and full doses of RA and Win caused an increase of *lpl* expression, whereas 60% treatment alone did not cause an increase. N, Combined treatments of both full and 50% DEAB and 60% Rimo caused a decrease of *lpl* expression, whereas respective treatments alone did not cause a significant decrease. *, $P < .05$ compared with control.

cyp26a1, a gene that targets RA for degradation and that is up-regulated in presence of RA. However, treatment with Win and Rimo did not influence the expression of *aldh1a2* or *cyp26a1* (Supplemental Figure 4, A–P). Similarly, RA and DEAB treatments did not alter the expression of *cb1* (Supplemental Figure 4, Q–T). Therefore, we were unable to establish a direct interaction of the two signaling pathways. Although an interaction was not observed, these experiments confirmed that the RA and ECS pathways have additive effects on lipid abundance and lipid metabolism.

RIGHTSLINK
The Endocrine Society. Downloaded from press.endocrine.org by [${individualUser.displayName}] on 19 May 2016. at 16:09 For personal use only. No other uses without permission. . All rights reserved.

Discussion

This study has shown that both the ECS- and RA-signaling pathway influence lipid abundance during zebrafish embryogenesis and that these actions can be combined to produce an enhanced effect. This combined effect, especially the effect that is caused in an additive manner of suboptimal doses, was important to establish because current clinical use of therapeutics that modulate these pathways are associated with toxic effects, which, in the case of Rimo has prevented its approval as an appetite regulator (52, 53). We further demonstrated that these pathways ameliorated the decrease of lipid levels caused by PPARγ inhibition, suggesting they lie downstream or are independent of this important regulator.

A key finding from this study was that the ECS and RA pathway could influence lipid deposition in vivo during embryogenesis. The activation of both the ECS and RA pathway led to an up-regulation of the lipoprotein lipase gene, which fits with the observed increases in lipid abundance marked by ORO, as lipoprotein lipase processes lipids within lipoproteins. A higher amount of lipoprotein lipase may therefore be required to process the increased abundance of lipids present in the embryos. Activation of the ECS has been shown to enhance increase *Lpl* expression (14) and lipogenesis in vitro (54), whereas ECS inhibition causes an increase in fatty acid oxidation (55). Increased lipogenesis could explain the increased lipid abundance detected in the embryos under ECS-activating treatments. It is unlikely that the increased lipid abundance is due to a decrease in fatty acid oxidation in our model, given that we did not detect a difference in oxygen consumption in the Win-treated embryos. In addition, it cannot be ruled out that the increased lipid abundance was caused by an increase of lipid trafficking from the yolk to the body. Furthermore, activation of the ECS has been shown to enhance adipocyte differentiation in vitro with corresponding increases in *Pparγ* expression (56, 57). It should be noted that in our model we were not measuring the presence or absence of adipocytes specifically, as in zebrafish they do not fully differentiate until 8 dpf at the earliest (31), although we were analyzing the presence of *c/ebpα* and *pparγ*, which could suggest the relative presence of preadipocyte cells.

The involvement of CB2 in controlling lipid abundance was unexpected, given that CB1 has been posited as the key receptor influencing lipid metabolism (17, 56, 58), whereas CB2 has been primarily identified as being involved in inflammation (59, 60). However, it has been shown that CB2 is expressed in mature human adipocytes (61). In addition, obese patients have higher circulating 2-AG levels (17), which has an equally high affinity for the CB2 receptor as it does for the CB1 receptor (62), indicating that a possible increase in CB2 activity is associated with total lipid levels. Furthermore, lipid production was shown to be induced by selective CB2 signaling in human sebocytes, which led to an increase in *Pparγ* expression (63). Our data are the first to demonstrate that the CB2 receptor can influence lipid abundance in vivo independent of the activity of CB1. Also, there should be no nonspecific activation of CB1 because the concentration of the selective CB2 agonist used in this study, Hu 308, was far below the binding affinity for CB1 (64). Therefore, we conclude that CB2 in conjunction with CB1 can influence lipid abundance in zebrafish during embryogenesis.

Because of the conflicting results reported on the effects of RA, having both pro- and antiadipogenic properties (23, 25, 28, 29), we performed an analysis of RA treatment on 3T3-L1 cells. Our results supported the findings by Kuri-Harcuch et al (25) showing an inhibition in adipocyte differentiation in 3T3-F442A cells. In line with their results, we saw this effect to be the strongest when cells were treated prior to differentiation. These results create an apparent contradiction to the effects that we observed when we treated our zebrafish embryos, where RA exposure caused an increase in lipid levels and *c/ebpα*, *fabp11a*, and *lpl* expression. However, the inhibitory effects of RA fit more with results reported by Berry et al (23), where RA was shown to prevent adipocyte differentiation in diet-induced obese mice through an increase in expression of *Kruppel-like factor 2*, *Sox9*, *and Pref-1*. The discrepancy of the effect of RA on lipid abundance could be an outcome of differences between mature adult cell lines and the cells of an embryo. For example, Li et al (65) showed that the neckless zebrafish mutant, which lacks a functional *aldh1a2*, had reduced lipid content in the pharyngeal arches due to cranial neural crest fate changes. Furthermore, RA is required at an early stage to differentiate embryonic stem cells into mature adipocytes (66). These previously reported findings and our results suggest differing roles for RA to enhance lipid abundance during embryogenesis and to inhibit adipocyte differentiation in mature cells. To further assess whether RA truly acts differently during embryogenesis and in the adult organism, other species could be studied during development under exposure to RA. Furthermore, adult zebrafish could be monitored under exposure to RA to understand whether this is a species-specific effect.

There has been only one previous publication to show a link between these the ECS and RA signaling. It was identified that RARγ binds to the promoter of *Cb1* in mouse hepatocytes and when activated increased its expression (67). However, that study did not investigate lipid quantity or lipid-associated gene expression in liver

RIGHTSLINK
The Endocrine Society. Downloaded from press.endocrine.org by [${individualUser.displayName}] on 19 May 2016. at 16:09 For personal use only. No other uses without permission. . All rights reserved.

cells. In our analysis, we were unable to observe a direct interaction with regard to changes in gene expression caused by modulation of either of the pathways. However, for monitoring the ECS, the expression of one receptor may not suggest a change in overall signaling activity, as the expression of a single receptor within a complex signaling pathway is not a comprehensive indicator of the activity of that pathway. Although, the combined influence on lipid abundance suggests a potential interaction, but it is possible that these two pathways work independently to influence the expression of *lpl* and *c/ebpα* and increase lipid abundance in the developing embryo.

Another interesting outcome of our study was that the two pathways ameliorated the negative effects caused by PPARγ inhibition. Because PPARγ plays a role in lipid metabolism, our aim was to determine the effects of the two pathways on lipid abundance with regard to PPARγ. Given that modulation of the ECS or RA signaling showed no effects on *pparγ* expression, but were able to increase ORO stain and *lpl* expression, these two pathways either act downstream or independently of PPARγ signaling. Interestingly, it has been shown in human primary adipocytes that activation of PPARγ with Rosi decreased the expression of *CB1* (68). Therefore, in our model, it is possible that decreased PPARγ activity increased *cb1* expression, which, combined with the ECS agonist, could have led to the increased lipid content.

The demonstrated effects on lipid abundance and gene expression caused by the interaction between the ECS and RA signaling may lead to a re-evaluation of the therapeutic potential of these drugs. Our results suggested that these pathways are viable targets to treat obesity. Additional experiments involving adult zebrafish or rodents could be conducted in the future to further elucidate the interactions of these pathways in mature and mammalian models. However, prior to now, associated toxic effects and other adverse effects have prevented the use of these drugs in humans (52, 53). Therefore, a dual prescription of these treatments at lower doses may be used to limit lipid abundance in obese patients while avoiding the off target/adverse effects associated with full posology of these drugs.

Acknowledgments

We thank the staff members of the Deakin University zebrafish facility for providing excellent husbandry care.

Address all correspondence and requests for reprints to: Dr Yann Gibert, Deakin University School of Medicine, 75 Pigdons Road, Waurn Ponds 3216, Australia. E-mail: y.gibert@deakin.edu.au.

Y.G. is supported by funding from the Centre for Molecular and Medical Research at Deakin University. S.L.M. is supported by a Career Development Fellowship from the National Health and Medical Research Council (1030474).

Disclosure Summary: The authors have nothing to disclose.

References

1. **Kelly T, Yang W, Chen CS, Reynolds K, He J.** Global burden of obesity in 2005 and projections to 2030. *Int J Obes*. 2008;32:1431–1437.
2. **Gesta S, Tseng YH, Kahn CR.** Developmental origin of fat: Tracking obesity to its source. *Cell*. 2007;131:242–256.
3. **Xiao J, Yang W.** Weight loss is still an essential intervention in obesity and its complications: A review. *J Obes*. 2012;2012:369097.
4. **Boden G, Shulman G.** Free fatty acids in obesity and type 2 diabetes: Defining their role in the development of insulin resistance and beta-cell dysfunction. *Eur J Clin Invest*. 2002;32:14–23.
5. **Calle EE, Thun MJ.** Obesity and cancer. *Oncogene*. 2004;23:6365–6378.
6. **Mariman EC.** Human biology of weight maintenance after weight loss. *J Nutrigenet Nutrigenomics*. 2012;5:13–25.
7. **Devane WA, Dysarz FA 3rd, Johnson MR, Melvin LS, Howlett AC.** Determination and characterization of a cannabinoid receptor in rat brain. *Molecular Pharmacology*. 1988;34:605–613.
8. **Munro S, Thomas KL, Abu-Shaar M.** Molecular characterization of a peripheral receptor for cannabinoids. *Nature*. 1993;365:61–65.
9. **Bermudez-Silva F, Viveros M, McPartland J, Rodriguez de Fonseca F.** The endocannabinoid system, eating behavior and energy homeostasis: The end or a new beginning. *Pharmacol Biochem Behav*. 2010;95:375–382.
10. **Kunos G, Osei-Hyiaman D, Liu J, Godlewski G, Bátkai S.** Endocannabinoids and the control of energy homeostasis. *World J Biol Chem*. 2008;283:33021–33025.
11. **Ryberg E, Larsson N, Sjögren S, et al.** The orphan receptor GPR55 is a novel cannabinoid receptor. *Br J Pharmacol*. 2007;152:1092–1101.
12. **Kapur A, Zhao P, Sharir H, et al.** Atypical responsiveness of the orphan receptor GPR55 to cannabinoid ligands. *World J Biol Chem*. 2009;284:29817–29827.
13. **Bensaid M, Gary-Bobo M, Esclangon A, et al.** The cannabinoid CB1 receptor antagonist SR141716 increases Acrp30 mRNA expression in adipose tissue of obese fa/fa rats and in cultured adipocyte cells. *Mol Pharmacol*. 2003;63:908–914.
14. **Cota D, Marsicano G, Tschöp M, et al.** The endogenous cannabinoid system affects energy balance via central orexigenic drive and peripheral lipogenesis. *J Clin Invest*. 2003;112:423–431.
15. **Karaliota S, Siafaka-Kapadai A, Gontinou C, Psarra K, Mavri-Vavayanni M.** Anandamide increases the differentiation of rat adipocytes and causes PPARgamma and CB1 receptor upregulation. *Obesity*. 2009;17:1830–1838.
16. **Matias I, Cristino L, Di Marzo V.** Endocannabinoids: Some like it fat (and sweet too). *J Neuroendocrinol*. 2008;20:100–109.
17. **Blüher M, Engeli S, Klöting N, et al.** Dysregulation of the peripheral and adipose tissue endocannabinoid system in human abdominal obesity. *Diabetes*. 2006;55:3053–3060.
18. **Duester G.** Retinoic acid synthesis and signaling during early organogenesis. *Cell*. 2008;134:921–931.
19. **Petkovich M, Brand NJ, Krust A, Chambon P.** A human retinoic acid receptor which belongs to the family of nuclear receptors. *Nature*. 1987;330:444–450.
20. **Chytil F, Ong DE.** Cellular retinol- and retinoic acid–binding proteins in vitamin A action. *Fed Proc*. 1979;38:2510–2514.

RIGHTSLINK
The Endocrine Society. Downloaded from press.endocrine.org by [${individualUser.displayName}] on 19 May 2016. at 16:09 For personal use only. No other uses without permission. . All rights reserved.

21. **Ray WJ, Bain G, Yao M, Gottlieb DI.** CYP26, a novel mammalian cytochrome P450, is induced by retinoic acid and defines a new family. *World J Biol Chem*. 1997;272:18702–18708.
22. **Mercader J, Ribot J, Murano I, et al.** Remodeling of white adipose tissue after retinoic acid administration in mice. *Endocrinology*. 2006;147:5325–5332.
23. **Berry DC, DeSantis D, Soltanian H, Croniger CM, Noy N.** Retinoic acid upregulates preadipocyte genes to block adipogenesis and suppress diet-induced obesity. *Diabetes*. 2012;61:1112–1121.
24. **Amengual J, Ribot J, Bonet ML, Palou A.** Retinoic acid treatment increases lipid oxidation capacity in skeletal muscle of mice. *Obesity*. 2008;16:585–591.
25. **Kuri-Harcuch W.** Differentiation of 3T3–F442A cells into adipocytes is inhibited by retinoic acid. *Differentiation*. 1982;23:164–169.
26. **Xue JC, Schwarz EJ, Chawla A, Lazar MA.** Distinct stages in adipogenesis revealed by retinoid inhibition of differentiation after induction of PPARgamma. *Mol Cell Biol*. 1996;16:1567–1575.
27. **Krupková M, Jank M, Liska F, et al.** Pharmacogenetic model of retinoic acid-induced dyslipidemia and insulin resistance. *Pharmacogenomics*. 2009;10:1915–1927.
28. **Morikawa K, Hanada H, Hirota K, Nonaka M, Ikeda C.** All-trans retinoic acid displays multiple effects on the growth, lipogenesis and adipokine gene expression of AML-I preadipocyte cell line. *Cell Biol Int*. 2013;37:36–46.
29. **Safonova I, Darimont C, Amri EZ, et al.** Retinoids are positive effectors of adipose cell differentiation. *Mol Cell Endocrinol*. 1994;104:201–211.
30. **De Botton S, Dombret H, Sanz M, et al.** Incidence, clinical features, and outcome of all trans-retinoic acid syndrome in 413 cases of newly diagnosed acute promyelocytic leukemia. The European APL Group. *Blood*. 1998;92:2712–2718.
31. **Flynn EJ 3rd, Trent CM, Rawls JF.** Ontogeny and nutritional control of adipogenesis in zebrafish (Danio rerio). *J Lipid Res*. 2009;50:1641–1652.
32. **Miyares RL, de Rezende VB, Farber SA.** Zebrafish yolk lipid processing: A tractable tool for the study of vertebrate lipid transport and metabolism. *Dis Model Mech*. 2014;7:915–927.
33. **Schlegel A, Stainier DY.** Microsomal triglyceride transfer protein is required for yolk lipid utilization and absorption of dietary lipids in zebrafish larvae. *Biochemistry*. 2006;45:15179–15187.
34. **Howe K, Clark MD, Torroja CF, et al.** The zebrafish reference genome sequence and its relationship to the human genome. *Nature*. 2013;496:498–503.
35. **Schlegel A, Gut P.** Metabolic insights from zebrafish genetics, physiology, and chemical biology. *Cell Mol Life Sci*. 2015:1–12.
36. **Ferré P.** The biology of peroxisome proliferator-activated receptors: Relationship with lipid metabolism and insulin sensitivity. *Diabetes*. 2004;53:S43–S50.
37. **Schoonjans K, Peinado-Onsurbe J, Lefebvre AM, et al.** PPARalpha and PPARgamma activators direct a distinct tissue-specific transcriptional response via a PPRE in the lipoprotein lipase gene. *EMBO J*. 1996;15:5336–5348.
38. **Kimmel CB, Ballard WW, Kimmel SR, Ullmann B, Schilling TF.** Stages of embryonic development of the zebrafish. *Dev Dyn*. 1995;203:253–310.
39. **Thisse C, Thisse B.** High-resolution in situ hybridization to whole-mount zebrafish embryos. *Nat Protoc*. 2007;3:59–69.
40. **Lyons SE, Shue BC, Lei L, Oates AC, Zon LI, Liu PP.** Molecular cloning, genetic mapping, and expression analysis of four zebrafish *c/ebp* genes. *Gene*. 2001;281:43–51.
41. **Thisse B, Thisse C.** Fast release clones: A high throughput expression analysis. *ZFIN Direct Data Submission*, 2004.
42. **Thisse C, Thisse B.** Expression from: Unexpected novel relational links uncovered by extensive developmental profiling of nuclear receptor expression. *ZFIN Direct Data Submission* 2008.
43. **Zizioli D, Forlanelli E, Guarienti M, et al.** Characterization of the AP-1 μ1A and μ1B adaptins in zebrafish (Danio rerio). *Dev Dyn*. 2010;239:2404–2412.
44. **Gibert Y, Gajewski A, Meyer A, Begemann G.** Induction and prepatterning of the zebrafish pectoral fin bud requires axial retinoic acid signaling. *Development*. 2006;133:2649–2659.
45. **Nishio S, Gibert Y, Berekelya L, et al.** Fasting induces CART downregulation in the zebrafish nervous system in a cannabinoid receptor 1-dependent manner. *Mol Endocrinol*. 2012;26:1316–1326.
46. **Xu F, Li K, Tian M, et al.** N-CoR is required for patterning the anterior-posterior axis of zebrafish hindbrain by actively repressing retinoid signaling. *Mech Dev*. 2009;126:771–780.
47. **Field HA, Ober EA, Roeser T, Stainier DY.** Formation of the digestive system in zebrafish. I. Liver morphogenesis. *Dev Biol*. 2003;253:279–290.
48. **Dudas J, Elmaouhoub A, Mansuroglu T, et al.** Prospero-related homeobox 1 (Prox1) is a stable hepatocyte marker during liver development, injury and regeneration, and is absent from "oval cells". *Histochem Cell Biol*. 2006;126:549–562.
49. **Wang ND, Finegold MJ, Bradley A, et al.** Impaired energy homeostasis in C/EBP alpha knockout mice. *Science*. 1995;269:1108–1112.
50. **Freytag SO, Paielli DL, Gilbert JD.** Ectopic expression of the CCAAT/enhancer-binding protein alpha promotes the adipogenic program in a variety of mouse fibroblastic cells. *Genes Dev*. 1994;8:1654–1663.
51. **Song Y, Selak MA, Watson CT, et al.** Mechanisms underlying metabolic and neural defects in zebrafish and human multiple acyl-CoA dehydrogenase deficiency (MADD). *PloS One*. 2009;4:e8329.
52. **Topol EJ, Bousser MG, Fox KA, et al.** Rimonabant for prevention of cardiovascular events (CRESCENDO): A randomised, multicentre, placebo-controlled trial. *Lancet*. 2010;376:517–523.
53. **Frankel SR, Eardley A, Lauwers G, Weiss M, Warrell RP.** The "retinoic acid syndrome" in acute promyelocytic leukemia. *Ann Intern Med*. 1992;117:292–296.
54. **Bellocchio L, Cervino C, Vicennati V, Pasquali R, Pagotto U.** Cannabinoid type 1 receptor: Another arrow in the adipocytes' bow. *J Neuroendocrinol*. 2008;20:130–138.
55. **Jbilo O, Ravinet-Trillou C, Arnone M, et al.** The CB1 receptor antagonist rimonabant reverses the diet-induced obesity phenotype through the regulation of lipolysis and energy balance. *FASEB J*. 2005;19:1567–1569.
56. **Matias I, Gonthier MP, Orlando P, et al.** Regulation, function, and dysregulation of endocannabinoids in models of adipose and beta-pancreatic cells and in obesity and hyperglycemia. *J Clin Endocrinol*. 2006;91:3171–3180.
57. **Bouaboula M, Hilairet S, Marchand J, Fajas L, Le Fur G, Casellas P.** Anandamide induced PPARgamma transcriptional activation and 3T3–L1 preadipocyte differentiation. *Eur J Pharmacol*. 2005;517:174–181.
58. **Di Marzo V.** CB(1) receptor antagonism: Biological basis for metabolic effects. *Drug Discov Today*. 2008;13:1026–1041.
59. **Steffens S, Veillard NR, Arnaud C, et al.** Low dose oral cannabinoid therapy reduces progression of atherosclerosis in mice. *Nature*. 2005;434:782–786.
60. **Klein TW, Newton C, Larsen K, et al.** The cannabinoid system and immune modulation. *J Leukoc Biol*. 2003;74:486–496.
61. **Roche R, Hoareau L, Bes-Houtmann S, et al.** Presence of the cannabinoid receptors, CB1 and CB2, in human omental and subcutaneous adipocytes. *Histochem Cell Biol*. 2006;126:177–187.
62. **Mallat A, Teixeira-Clerc F, Deveaux V, Manin S, Lotersztajn S.** The endocannabinoid system as a key mediator during liver diseases: New insights and therapeutic openings. *Br J Pharmacol*. 2011;163:1432–1440.
63. **Dobrosi N, Tóth BI, Nagy G, et al.** Endocannabinoids enhance

RIGHTSLINK
The Endocrine Society. Downloaded from press.endocrine.org by [${individualUser.displayName}] on 19 May 2016. at 16:09 For personal use only. No other uses without permission. . All rights reserved.

lipid synthesis and apoptosis of human sebocytes via cannabinoid receptor-2-mediated signaling. *FASEB J*. 2008;22:3685–3695.
64. **Hanus L, Breuer A, Tchilibon S, et al.** HU-308: A specific agonist for CB(2), a peripheral cannabinoid receptor. *Proc Natl Acad Sci U S A*. 1999;96:14228–14233.
65. **Li N, Kelsh RN, Croucher P, Roehl HH.** Regulation of neural crest cell fate by the retinoic acid and Pparg signalling pathways. *Development*. 2010;137:389–394.
66. **Field SJ, Johnson RS, Mortensen RM, Papaioannou VE, Spiegelman BM, Greenberg ME.** Growth and differentiation of embryonic stem cells that lack an intact c-fos gene. *Proc Natl Acad Sci U S A*. 1992; 89:9306–9310.
67. **Mukhopadhyay B, Liu J, Osei-Hyiaman D, et al.** Transcriptional regulation of cannabinoid receptor-1 expression in the liver by retinoic acid acting via retinoic acid receptor-gamma. *World J Biol Chem*. 2010;285:19002–19011.
68. **Pagano C, Pilon C, Calcagno A, et al.** The endogenous cannabinoid system stimulates glucose uptake in human fat cells via phosphatidylinositol 3-kinase and calcium-dependent mechanisms. *J Clin Endocrinol*. 2007;92:4810–4819.

RIGHTSLINK
The Endocrine Society. Downloaded from press.endocrine.org by [${individualUser.displayName}] on 19 May 2016. at 16:09 For personal use only. No other uses without permission. . All rights reserved.